THE ASTROPHYSICAL JOURNAL SUPPLEMENT SERIES, 59:499–511, 1985 December

VLA MAPS OF 41 RADIO GALAXIES

R. R. J. ANTONUCCI
National Radio Astronomy Observatory,[1] Charlottesville, Virginia
Received 1985 January 14; accepted 1985 June 19

ABSTRACT

Forty-one radio galaxies have been mapped at 6 cm with the VLA in its B-configuration. Good dynamic range has been achieved by application of a self-calibration program.

Subject headings: radio sources: galaxies

I. INTRODUCTION

This paper is a by-product of a major project to study the relationship between the optical and radio properties of radio galaxies. Forty-seven objects were observed with the VLA to provide the necessary radio data. Paper I (Antonucci 1984*a*) presents optical spectropolarimetry data, and discusses the relationship of the optical polarization position angles to the symmetry axes of the associated radio sources. Paper II (Antonucci 1984*b*) contains a statistical study of the relationship of optical spectroscopic and morphological properties to radio properties for a large sample of radio galaxies. The radio maps made for those studies can be used by other astronomers for many different purposes, so I am placing them in the literature in this paper. Selection criteria for mapping were complicated, including the prior availability of a good map in the literature, and the availability of spectroscopic data from Lick Observatory. Information on the vast majority of the radio galaxies can be found in Burbidge and Crowne (1979, hereafter "the catalog"). In particular, that catalog contains fairly complete information or redshifts, optical magnitudes, optical positions, and 408 MHz integrated radio flux densities.

II. OBSERVATIONS

The observations were made on 1981 May 1 with almost all of the VLA antennas in their B-array positions (Thompson *et al.* 1980). The maps were made from "two-cut snapshots": two brief integrations separated by a few hours. The integrations were typically 6 minutes long, and each was preceded and followed by an observation of a nearby VLA phase calibrator. The whole procedure was performed at 4.535 and at 4.985 GHz separately, using 50 MHz bandwidths. Then the two visibility data bases were combined to obtain better sensitivity and *U-V* plane coverage. The maps made with the combined data set have an effective frequency of ~ 4.760 GHz. Flux (and polarization) calibration was performed in the standard way, using concurrent observations of 3C 138 and 3C 286.

All of the maps were made in much the same way. Typically the mapper-cleaner program MX in the NRAO AIPS data processing package was used to make 256×256 cell maps, with map cell sizes of 0″.4. All but the outermost few pixels were included in the "clean window." The visibilities were tapered to reduce their weighting to 30% at 200,000 wavelengths (200 kλ), basically eliminating the few long A-array spacings. The tapering improved the map dynamic ranges. In most cases three iterations of the self-calibration routine ASCAL were performed, a phase calibration followed by two passes correcting both amplitudes and phases. For the strongest sources the resulting dynamic ranges are > 200 to 1, with dynamic range defined as map peak divided by three times map rms noise. The dynamic range on weak sources is limited by the thermal noise, which is ~ 150 μJy rms per beam.

These maps misrepresent the true source brightness distribution in one serious way. For all but the smallest sources, substantial flux density on long spatial scales has been resolved out by these high-resolution observations. The data are not well suited to mapping large, smooth, steep spectrum lobes. In addition to the 41 successful maps, data were taken on several objects with so much very large scale flux that good maps could not be made. These sources are 3C 98, 3C 192, 3C 227, 3C 445, and 4C 25.60. One source, 3C 459, has been excluded because excellent maps have been published by Ulvestad (1985).

Since the maps are at high frequency and of high resolution, they are most suitable for detecting relatively compact and flat-spectrum features, namely, cores, jets, and hot spots. Objects in which only a core was detected are not shown. Their positions and flux densities are provided in Table 1. Position errors are estimated at 0″.1, and flux density errors are expected to be ± 5%. The remaining 35 objects are shown in Figures 1–35. Almost all of the maps are tapered at 200 kλ as described above, resulting in beam sizes $\sim 1''.6$ (see Table 2). In almost all cases the highest contour level shown is 0.88 times the map peak, and the other levels are down by successive factors of $\sqrt{2}$. Exceptions are indicated in § III. Where possible, a vertical bar of length 20 kpc ($H_0 = 75$ km s^{-1} Mpc^{-1}, $q_0 = \frac{1}{2}$) has been drawn on each figure. Several maps were too small to accommodate 20 kpc bars. At the distance of NGC 828 (Fig. 4), 20 kpc corresponds to 58″.8; for 3C 305 (Fig. 23), 20 kpc equals 27″.0; and for NGC 6240 (Fig. 29), 20 kpc corresponds to 43″.2. No scale bars are shown for 0207+095, 0446−206, 3C 178, and 4C 14.37, because no redshifts are available for them.

[1] The National Radio Astronomy Observatory is operated by Associated Universities, Inc., under contract with the National Science Foundation.

TABLE 1

UNRESOLVED SOURCES

OBJECT	POSITION R.A. (1950)	POSITION DECL. (1950)	FLUX AT 4.76 GHz (Jy)
B2 0648+275	$6^h48^m54\overset{s}{.}83$	$+27°31'18\overset{''}{.}2$	0.213
PKS 0723−008	7 23 17.84	−0 48 55.4	1.91
4C 48.29[a]	10 17 47.65	+48 46 31.0	0.036
NGC 5077	13 16 52.92	−12 23 40.9	0.100
4C 12.50	13 45 6.17	+12 32 20.2	2.93
4C 39.49 = Mrk 501	16 52 11.72	+39 50 25.3	1.25

[a] There is no secure optical identification. The identification reference in Burbidge and Crowne 1979 is Bailey and Pooley 1968. That paper only mentions "two 17 mag. interacting galaxies" at $10^h17^m20^s$, 48°46′20″. Bailey and Pooley also note that 4C 48.29 consists of two extended radio components, at $10^h17^m50\overset{s}{.}1 \pm 2\overset{s}{.}0$, 48°47′39″ ± 10″ and at $10^h17^m50\overset{s}{.}1 \pm 2\overset{s}{.}0$, 48°43′27″ ± 10″. Perhaps these extended components are double radio lobes, resolved out by the present observation, and associated with the core observed here.

TABLE 2

BEAM SIZES

Figure	IAU Designation	Object	Beam Size (arcsec)	Beam Position Angle (degrees)
1	0039+400	5C 3.100	1.65×1.40	−5.86
2	0123−016	3C 40	3.26×3.26	44.61
3	0204+292	4C 29.06	2.25×2.08	56.86
4	0206+355	4C 35.03	1.68×1.50	8.85
5	0207+389	NGC 828	2.03×1.99	46.55
6	0207+095	PKS	1.78×1.56	−24.87
7	0307+169	3C 79	1.61×1.57	−39.94
8	0343+700	4CT 69.05.1	2.42×1.37	−89.70
9	0410+110	3C 109	2.63×2.08	−52.96
10	0446−206	PKS	2.56×1.04	4.62
11	0456−043	4C −04.17	1.94×1.29	1.78
12	0651+542	3C 171	1.59×1.53	−66.04
13	0722−095	3C 178	1.97×1.43	−15.28
14	0755+379	NGC 2484	1.56×1.47	21.35
15	0906−094	MC	2.13×1.32	−10.50
16	1043+140	4C 14.37	3.23×2.48	58.14
17	1057+744	4C 74.17	1.86×1.30	16.88
18	1113+295	4C 29.41	2.03×1.67	70.84
19*a*	1330+022	3C 287.1	2.00×1.59	19.84
19*b*	1330+022	3C 287.1	4.13×3.81	0.00
20	1358−113	PKS	7.54×7.54	45.00
21	1359+025	4C 02.39	1.90×1.54	18.62
22	1417−192	PKS	1.87×1.40	27.70
23	1448+634	3C 305	1.00×1.00	0.00
24*a*	1453+120	MC2	1.00×1.00	0.00
24*b*	1453+120	MC2	4.08×3.90	17.46
25	1514+072	3C 317	1.87×1.53	16.89
26	1531+359	4C 35.37	1.62×1.56	−3.74
27	1559+021	3C 327	4.39×3.88	2.08
28	1615+324	3C 332	4.07×3.83	16.38
29	1650+024	NGC 6240	1.99×1.55	−0.11
30	1832+474	3C 381	1.53×1.46	27.75
31	1833+326	3C 382	4.03×3.97	59.26
32*a*	2201+044	4C 04.77	1.90×1.42	3.02
32*b*	2201+044	4C 04.77	4.10×3.83	1.88
33*a*	2243+394	3C 452	3.77×3.77	45.00
33*b*	2243+394	3C 452	7.54×7.54	45.00
34	2322−123	PKS	2.29×1.35	−3.30
35	2349−014	4C −01.61	2.03×1.40	−5.58

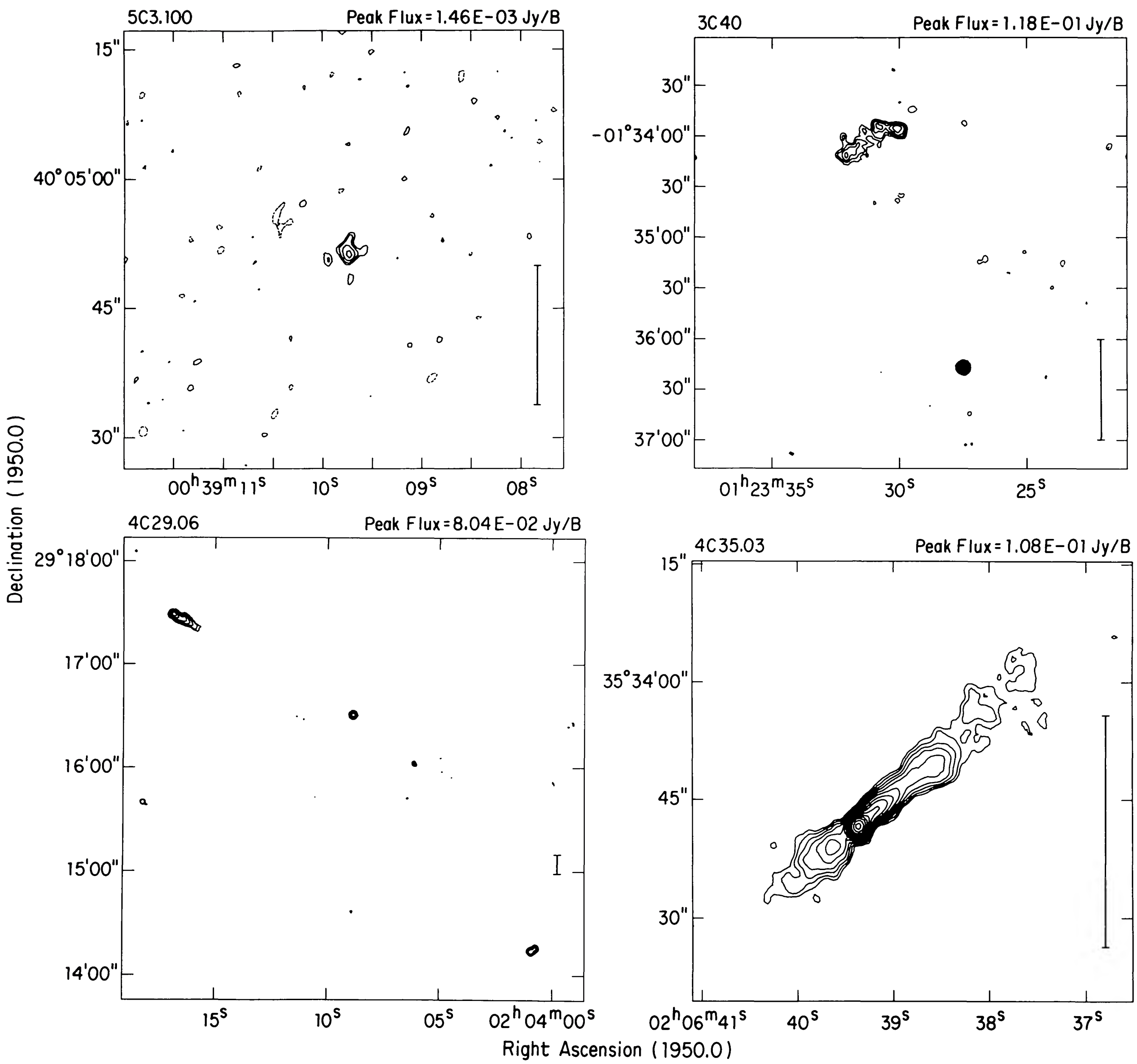

FIGS. 1–4

FIGS. 1–35.—Six centimeter VLA maps of radio galaxies. Unless noted otherwise, each map was made with visibilities tapered to 30% weight at 200,000 wavelengths. Beam sizes are listed in Table 2, 1″.6 being typical for the high-resolution, 200 kλ taper maps. Figures on each page are displayed in numerical order, from left to right and from top to bottom. Figs. 1–4: 5C 3.100, 3C 40, 4C 29.06, 4C 35.03.

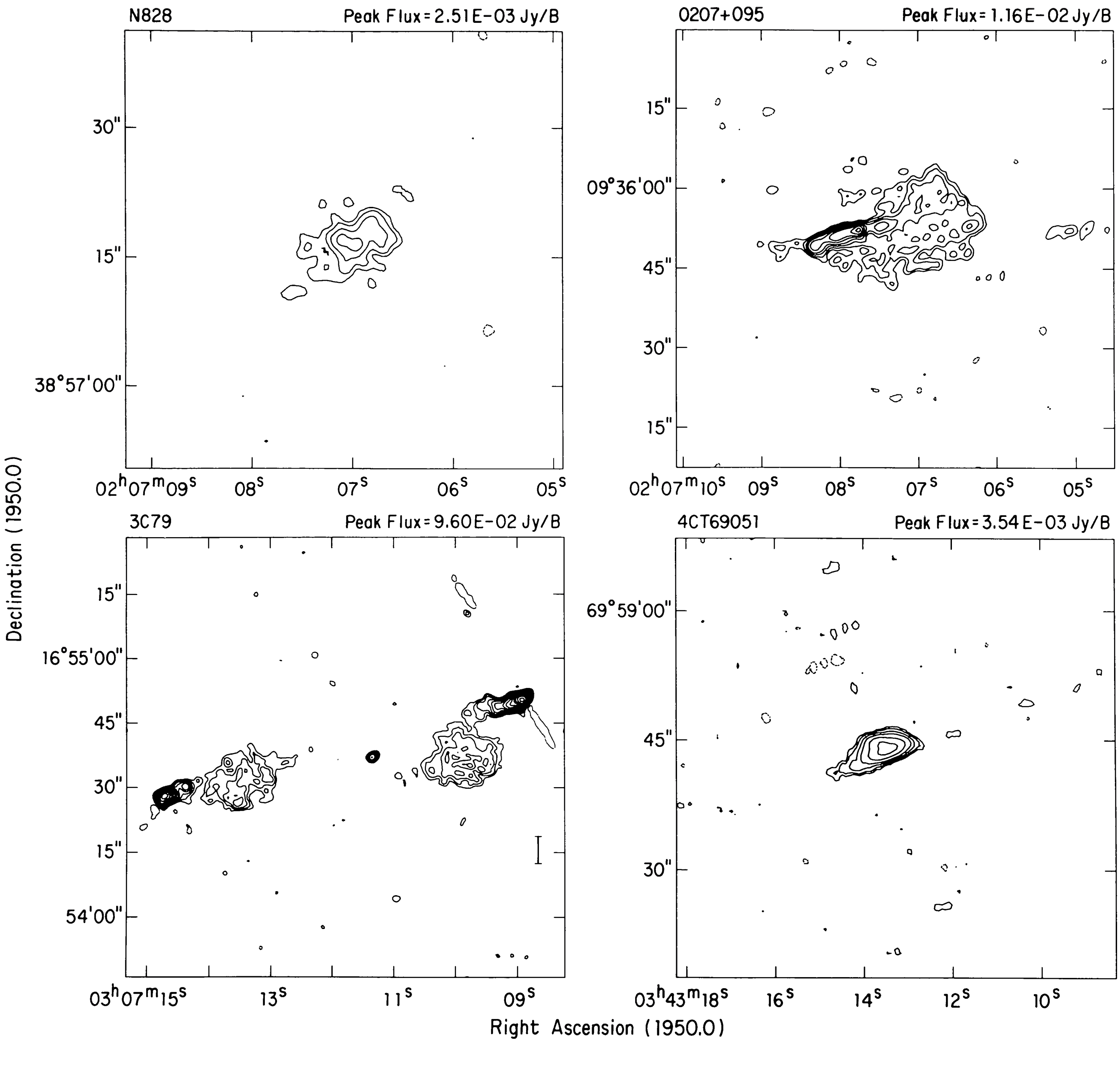

FIGS. 5–8.—NGC 828, 0207+095, 3C 79, 4CT 69.05.1

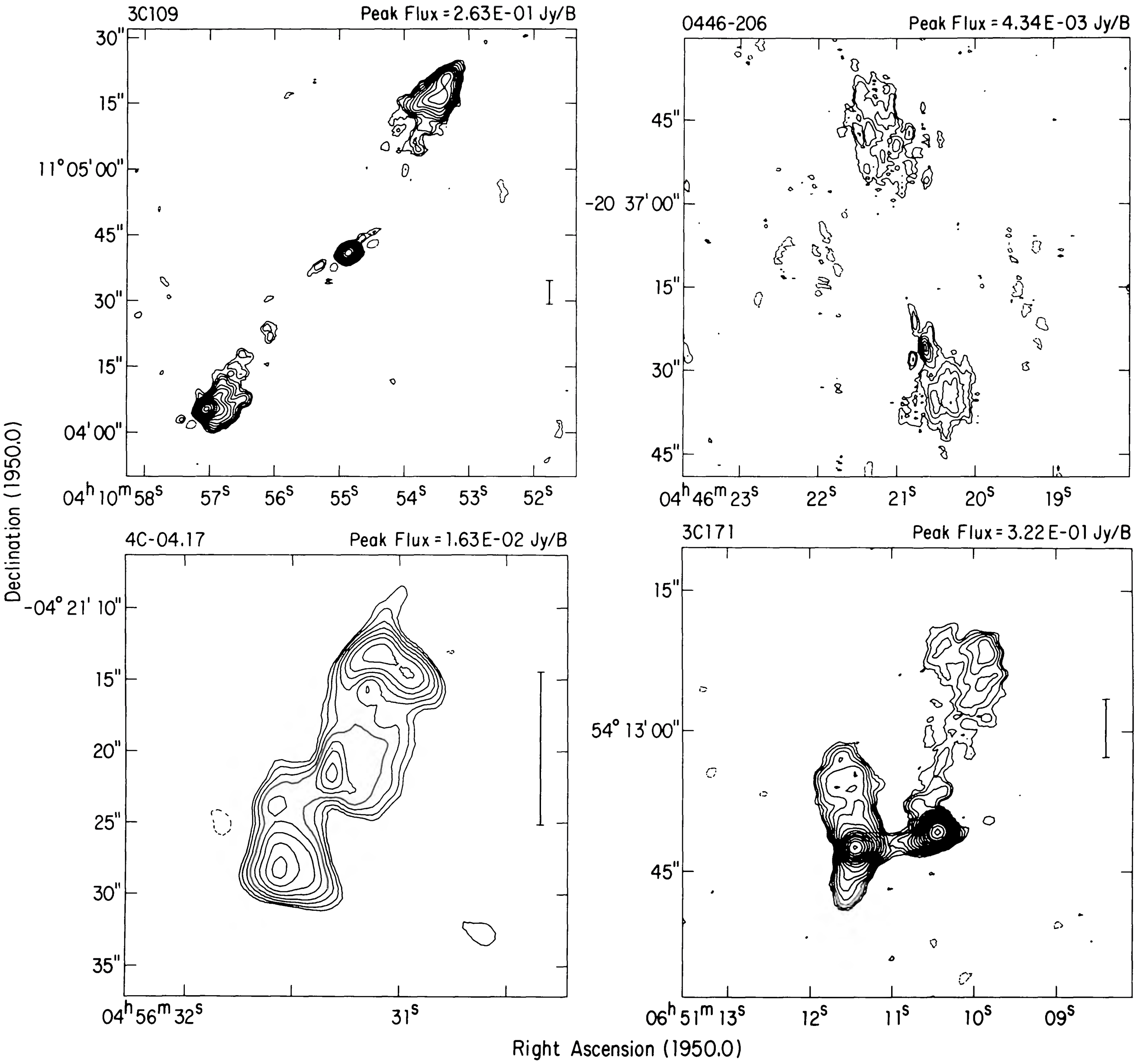

FIGS. 9–12.—3C 109, 0446–206, 4C –04.17, 3C 171

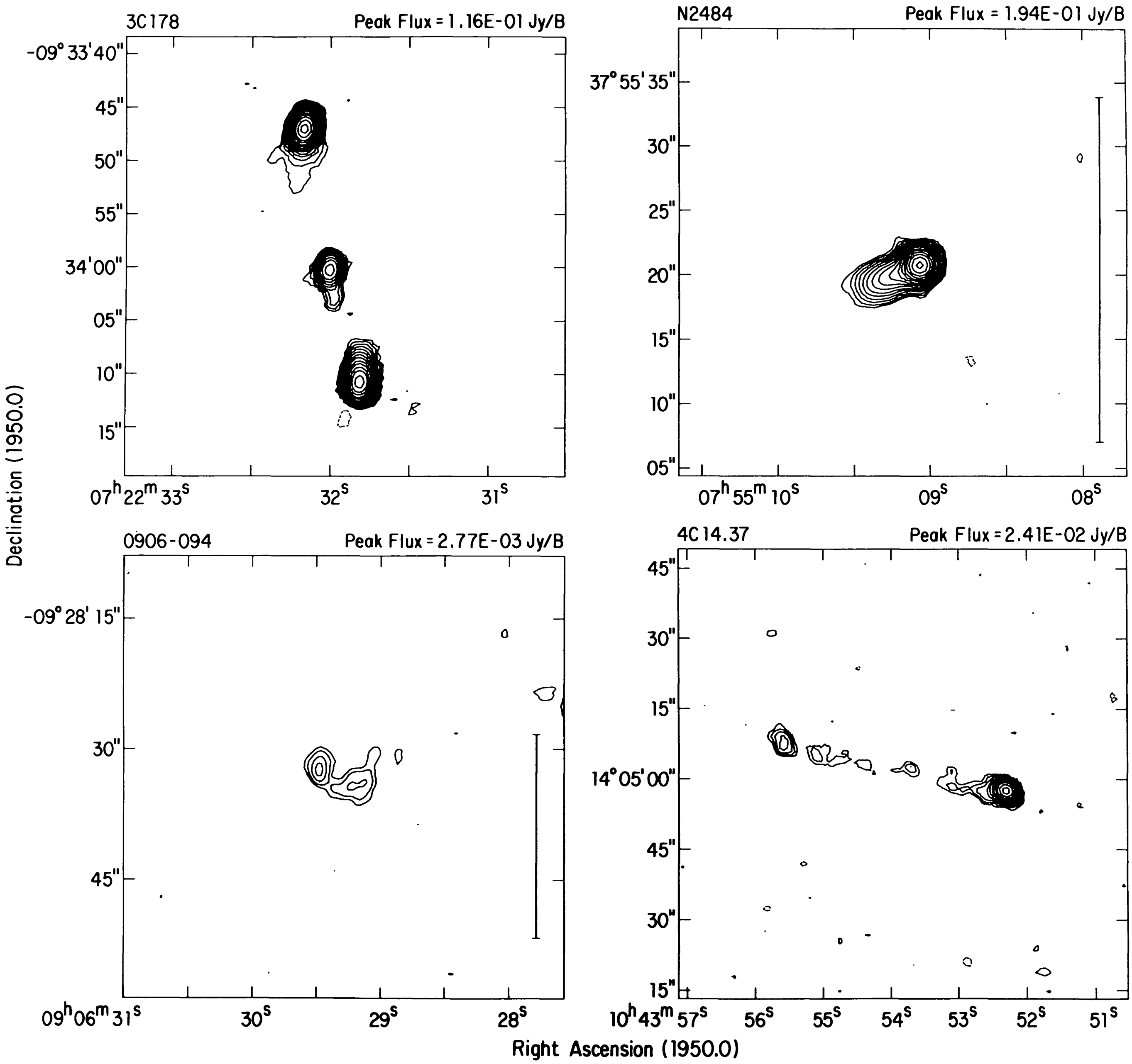

FIGS. 13–16.—3C 178, NGC 2484, 0906−094, 4C 14.37

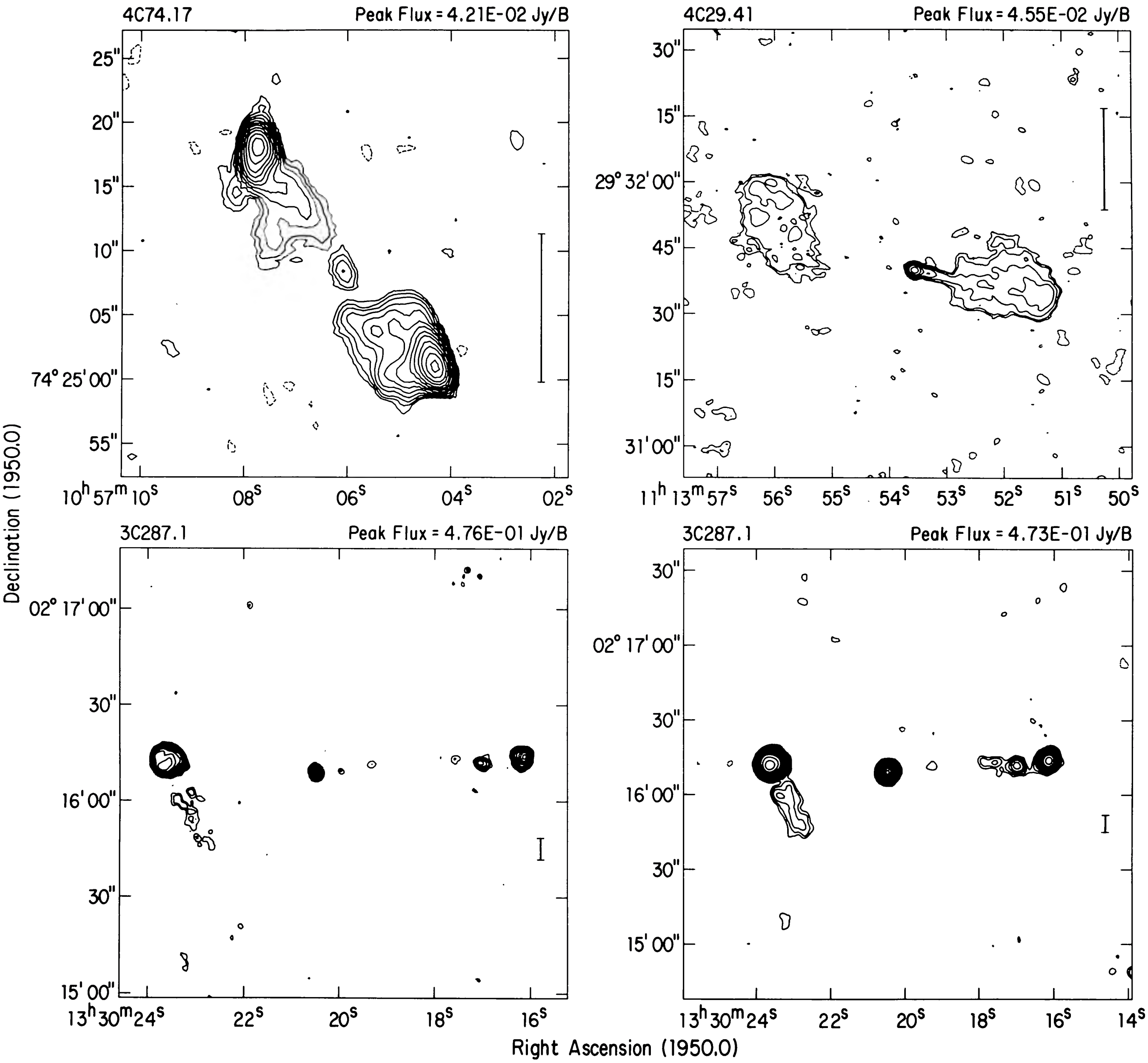

FIGS. 17, 18, 19*a*, 19*b*.—4C 74.17, 4C 29.41, 3C 287.1, 3C 287.1 (larger beam size)

1985ApJS...59..499A

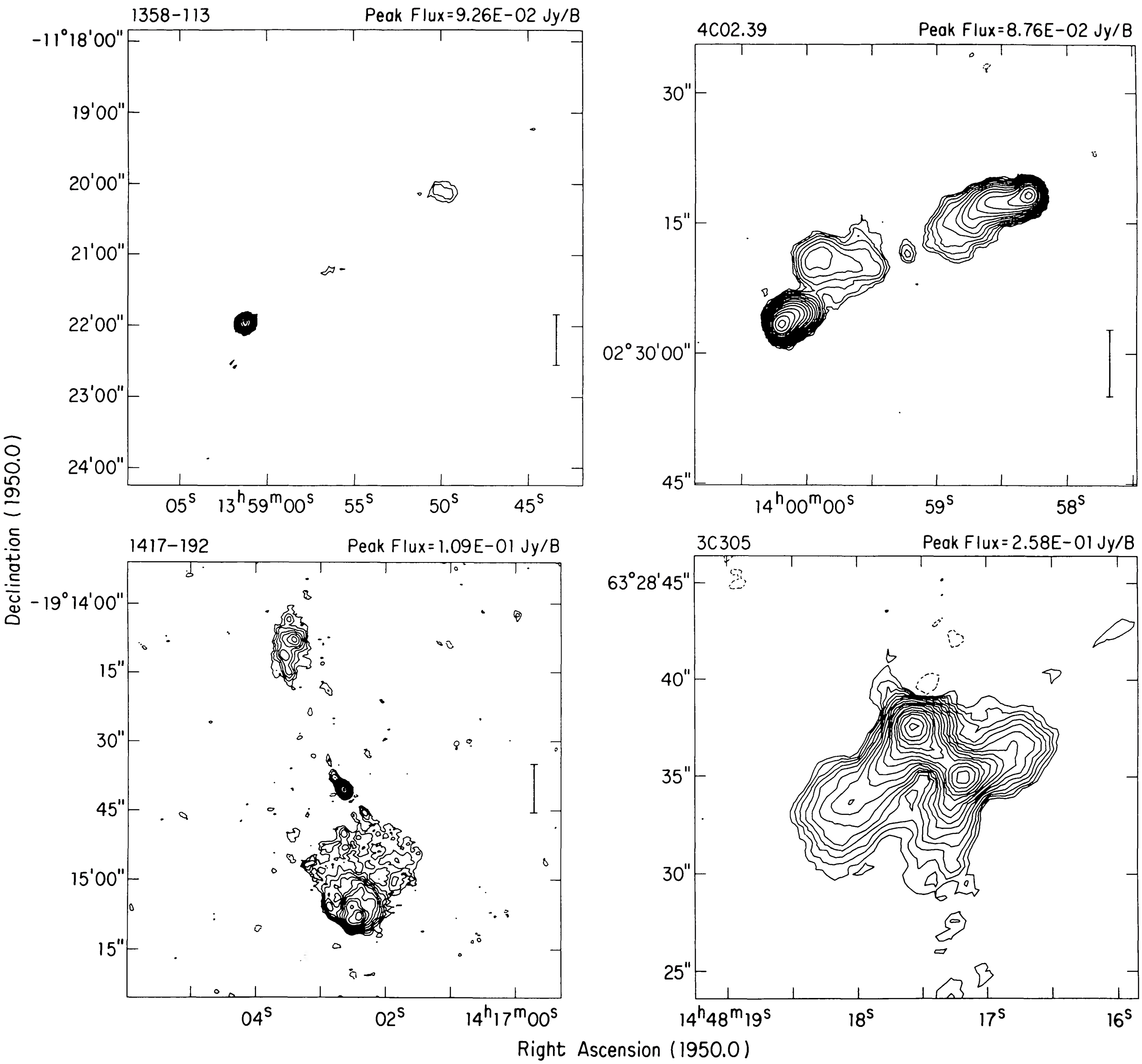

FIGS. 20–23.—1358−113, 4C 02.39, 1417−192, 3C 305

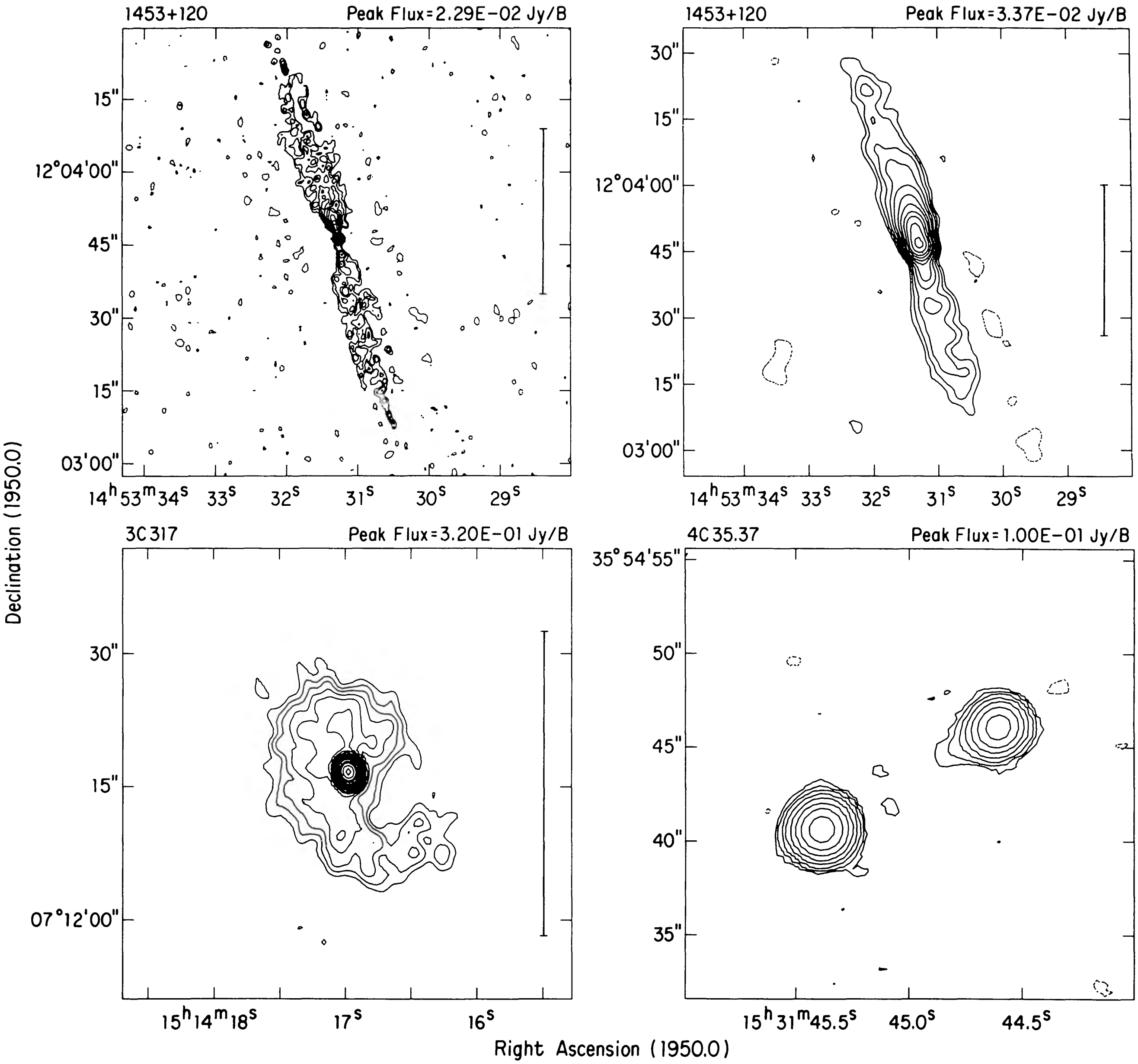

FIGS. 24*a*, 24*b*, 25, 26.—1453+120, 1453+120 (larger beam size), 3C 317, 4C 35.37

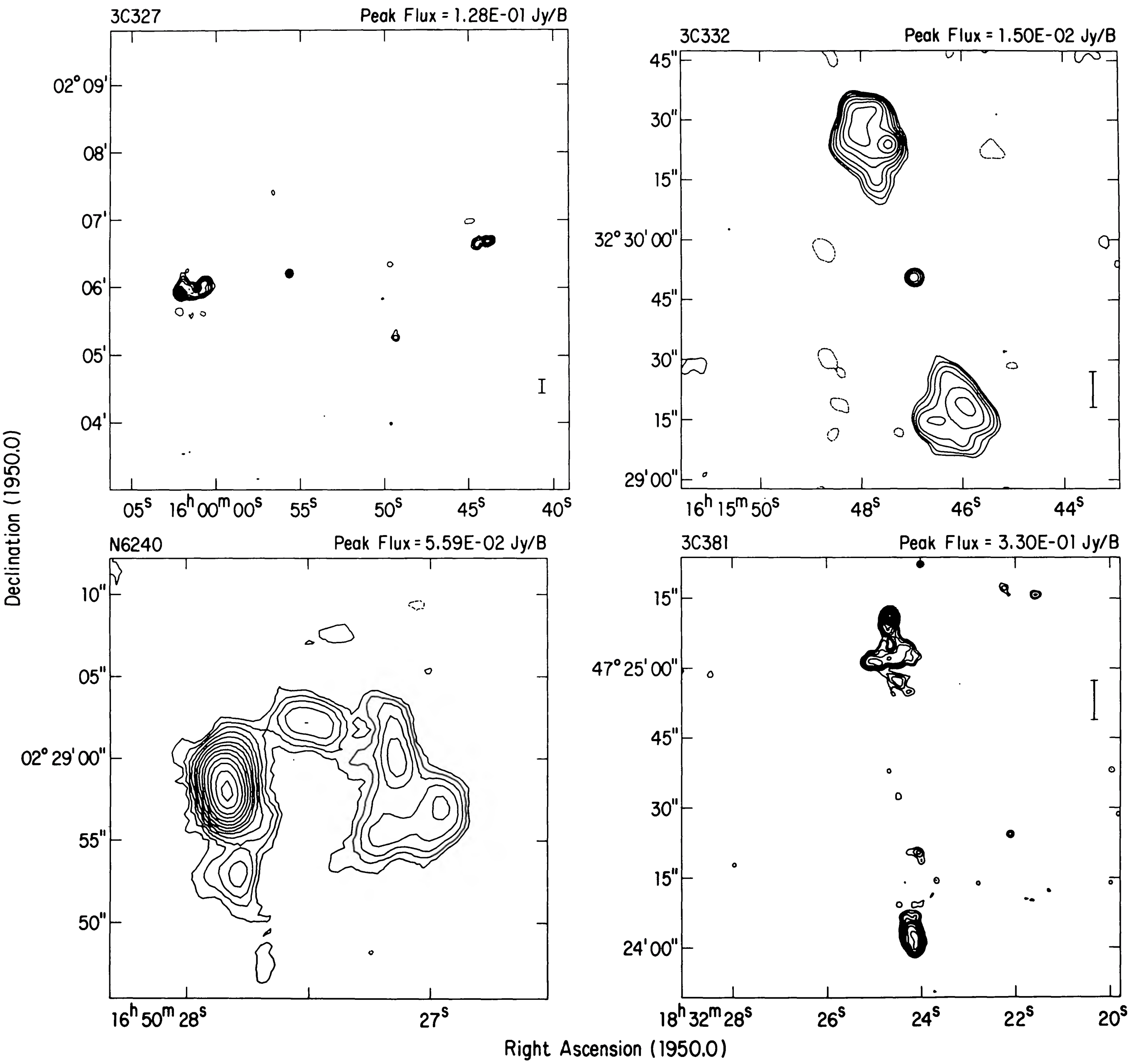

FIGS. 27–30.—3C 327, 3C 332, NGC 6240, 3C 381

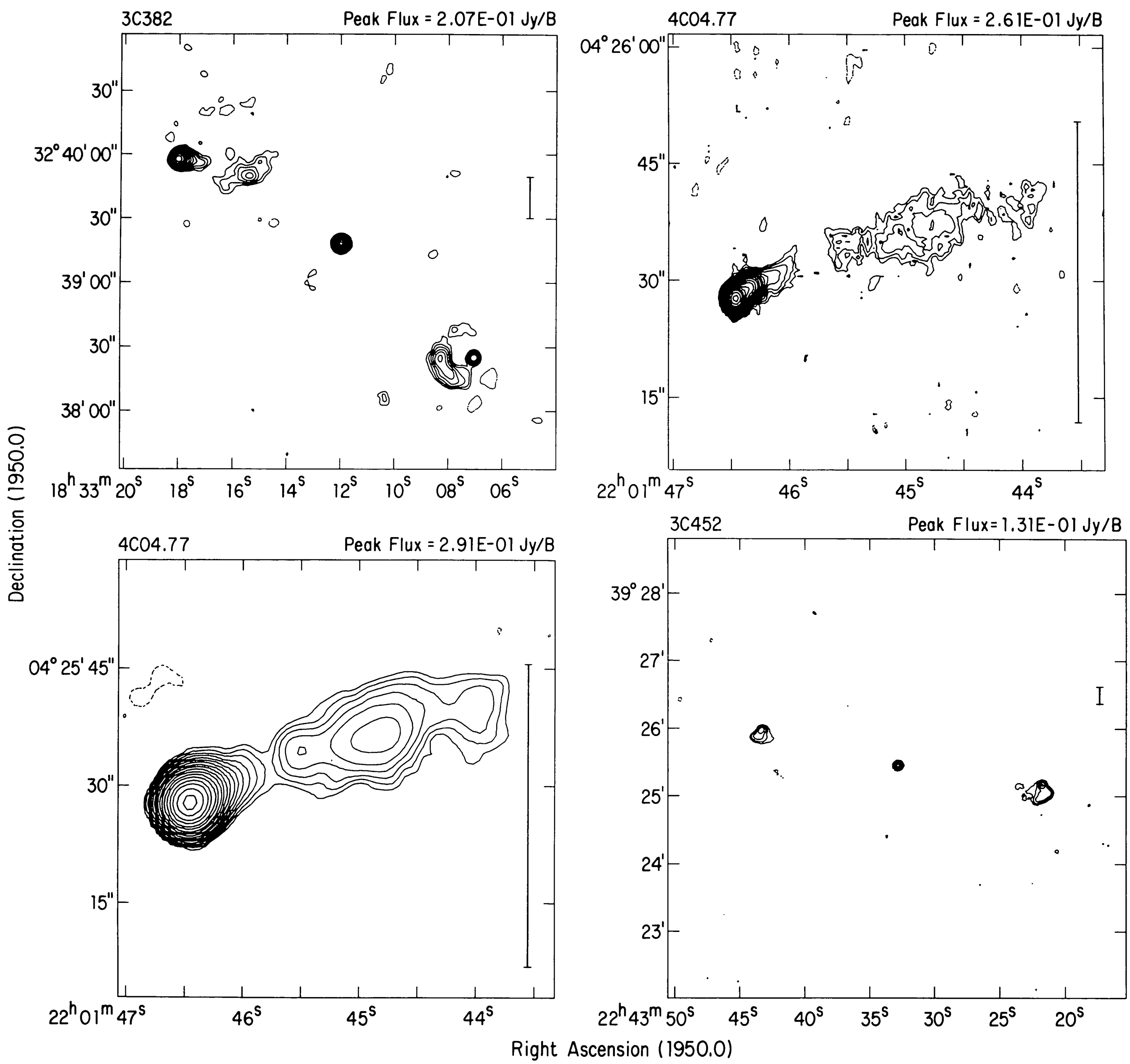

FIGS. 31, 32*a*, 32*b*, 33*a*.—3C 382, 4C 04.77, 4C 04.77 (larger beam size), 3C 452

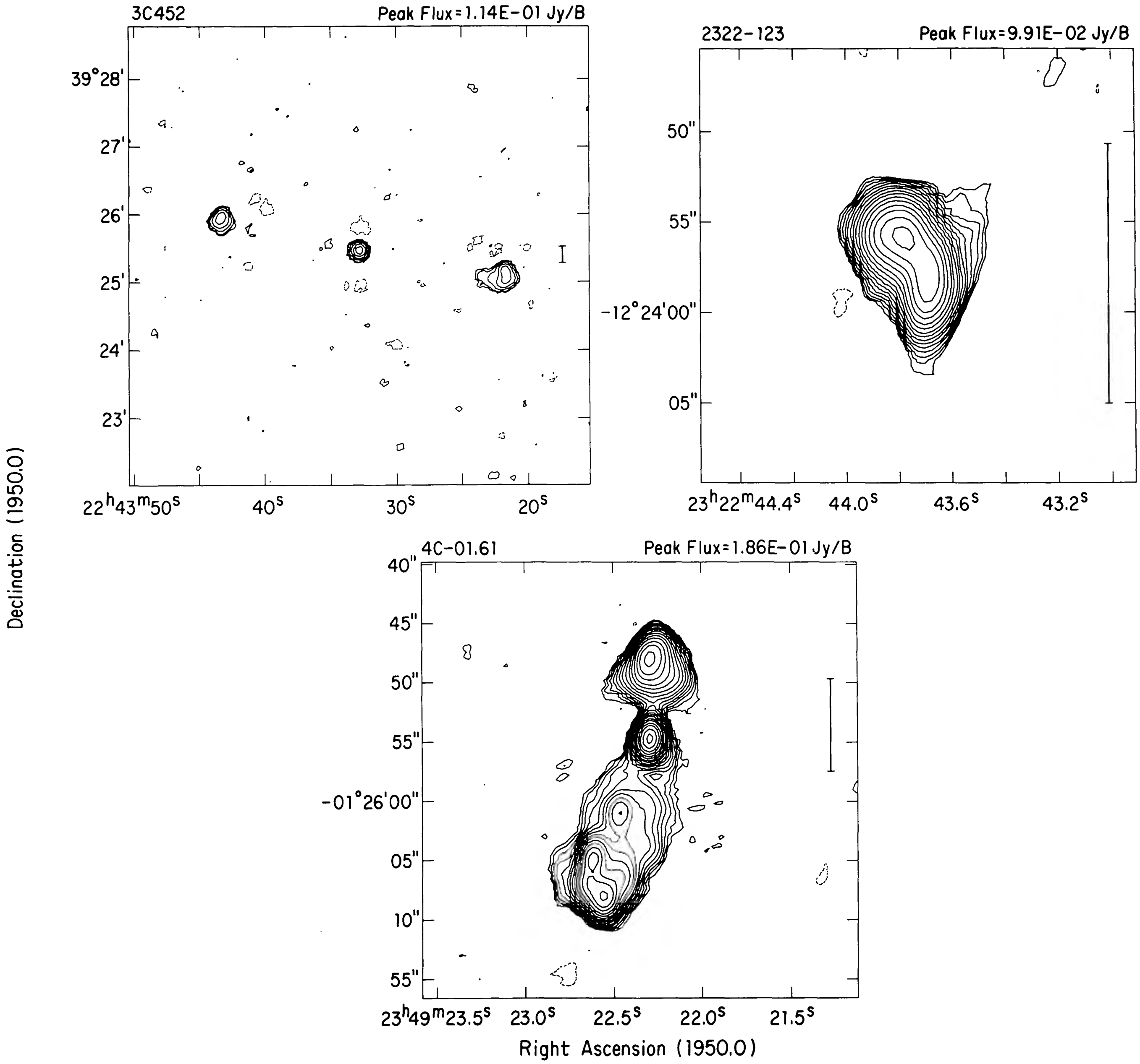

FIGS. 33*b*, 34, 35.—3C 452 (larger beam size than in Fig. 33*a*), 2322−123, 4C −01.61

An optical position with an accuracy of a few arcseconds or better is available for most of these galaxies (Burbidge and Crowne 1979), and they are usually consistent with a prominent radio core on these maps. Obvious discrepancies or ambiguities are described in § III.

III. NOTES ON PARTICULAR MAPS

3C 40 (Fig. 2).—50 kλ taper. The point source is identified in the catalog with the NGC 545/547 pair. I have determined that the radio core is associated with NGC 547, on the basis of rough optical astrometry. It is not obvious how to relate this map to the low-resolution map of Schilizzi and McAdam (1975).

4C 29.06 (Fig. 3).—Contour levels at peak flux density times 0.64, 0.32, 0.16, 0.08, 0.04, 0.02, 0.014, and −0.014.

0207+095 (Fig. 6).—No redshift is available. Clark, Bolton, and Shimmins (1966) identify this with a galaxy at $2^h7^m8^s$, 9°36′.1. I find an image on the Palomar Observatory Sky Survey print, perhaps a faint galaxy plus a foreground star, at $2^h7^m7^s.83$, 9°35′50″.3, coincident with the radio core. My optical position errors are ~1″ in each coordinate.

4CT 69051 (Fig. 8).—The rough optical coordinates of a $V = 14.6$ spiral galaxy are given in the catalog as $3^h43^m18^s$, 70°0′, but I find that the galaxy is at approximately $3^h43^m13^s.6$, 69°58′43′, right on the radio source.

0446−206 (Fig. 10).—Mills and Hoskins (1977) find an optical galaxy at approximately $4^h46^m19^s.3$, −20°37′25″, but

I do not find anything obvious on the Sky Survey between the radio lobes, except for a faint stellar object at $4^h46^m20^s.69$, $-20°37'24''.3$.

3C 178 (Fig. 13).—The catalog optical identification for 3C 178, a galaxy at $7^h22^m33^s$, $-9°33'36''$, is incorrect (Haschick *et al.* 1980). There is nothing obvious at the radio core position on the Sky Survey.

NGC 2484 (Fig. 14).—The catalog redshift reference, Colla *et al.* (1975), gives $z = 0.0413$, so the catalog value is probably a typographical error.

4C 14.37 (Fig. 16).—100 kλ taper. The extended emission is parallel to a ridge in the dirty beam, so it is somewhat suspect. The catalog identification for 4C 14.37 is the bright galaxy NGC 3367, but this map shows that the radio source is far from the galaxy, whose position is given as $10^h43^m56^s$, $14°0'18''$ in Sandage and Tammann (1981). There is nothing obvious at the radio core position on the Sky Survey.

4C 29.41 (Fig. 18).—Contour levels at peak flux density times 0.64, 0.32, 0.16, 0.08, 0.04, 0.02, 0.014, and −0.014.

3C 287.1 (Fig. 19*b*).—40 kλ taper.

1358−113 (Fig. 20).—40 kλ taper. The extended emission is parallel to a ridge in the dirty beam, so it is somewhat suspect. The redshift of 1358−113 is considered uncertain by Burbidge and Crowne (1979).

1453+120 (Figs. 24*a*, 24*b*).—The redshift of 1453+120 is considered uncertain by Burbidge and Crowne (1979). A 40 kλ taper has been applied to Figure 14*b*.

4C 35.37 (Fig. 26).—Contour levels at peak flux density times 0.64, 0.32, 0.16, 0.08, 0.04, 0.02, 0.01, 0.005, and −0.005. The catalog optical position is $15^h31^m44^s.9$, $35°54'18''$, rather far from the radio source. I have measured the optical position of the N galaxy to be $15^h31^m45^s.12$, $35°54'21''.9$, with errors of $\sim 1''$, so the catalog identification is suspect.

3C 327 (Fig. 27).—40 kλ taper.

3C 332 (Fig. 28).—40 kλ taper.

NGC 6240 (Fig. 29).—The two apparent optical nuclei are at $16^h50^m27^s.96$, $2°29'55''.2$ and $16^h50^m29^s.98$, $2°29'57''.0$ according to Fried and Schulz (1983). These positions are right in the gap where there is no radio emission.

3C 381 (Fig. 30).—No radio core has been detected, but the catalog optical position is centered between the two lobes.

3C 382 (Fig. 31).—40 kλ taper.

4C 04.77 (Fig. 32*b*).—40 kλ taper.

3C 452 (Fig. 33*a*).—Contour levels at peak flux density times 0.64, 0.32, 0.16, 0.08, 0.04, 0.02, and −0.02. (Fig. 33*b*) 40 kλ taper. Contour levels at peak flux density times 0.64, 0.32, 0.16, 0.08, 0.04, 0.028, and −0.028.

REFERENCES

Antonucci, R. R. J. 1984*a*, *Ap. J.*, **278**, 499.
______. 1984*b*, *Ap. J.*, **281**, 112.
Bailey, J. A., and Pooley, G. G. 1968, *M.N.R.A.S.*, **138**, 51.
Burbidge, G., and Crowne, A. H. 1979, *Ap. J. Suppl.*, **40**, 583.
Clark, M. E., Bolton, J. G., and Shimmins, A. J. 1966, *Australian J. Phys.*, **19**, 375.
Colla, G., Fanti, C., Fanti, R., Gioia, I., Lari, C., Lequeux, J., Lucas, R., and Ulrich, M. H. 1975, *Astr. Ap. Suppl.*, **20**, 1.
Fried, J. W., and Schulz, H. 1983, *Astr. Ap.*, **118**, 166.
Haschick, A. D., Crane, P. C., Greenfield, P. E., Burke, B. F., and Baan, W. A. 1980, *Ap. J.*, **239**, 774.
Mills, B. Y., and Hoskins, D. G. 1977, *Australian J. Phys.*, **30**, 509.
Sandage, A., and Tammann, G. A. 1981, *A Revised Shapley-Ames Catalog of Bright Galaxies* (Carnegie Institution of Washington Pub. 635).
Schilizzi, R. T., and McAdam, W. B. 1975, *Mem. R.A.S.*, **79**, 1.
Thompson, A. R., Clark, B. G., Wade, C. M., and Napier, P. J. 1980, *Ap. J. Suppl.*, **44**, 151.
Ulvestad, J. S. 1985, *Ap. J.*, **288**, 514.

R. R. J. ANTONUCCI: Space Telescope Science Institute, Homewood Campus, Baltimore, MD 21218